BIOCOORDINATION, COMPUTATIONAL MODELING AND ANTIBACTERIAL SENSITIVITIES OF COBALT (II), NICKEL (II), COPPER (II) AND BISMUTH (V) WITH GENTAMICIN AND AMOXICILLIN ANTIBIOTICS MIXED LIGANDS

Parashuram Mishra
Department of Chemistry, University of Delhi, Delhi-110007, India
Email: prmmishra@rediffmail.com

ABSTRACT

A new ligand was made by coupling gentamicin and amoxicillin. It is proposed that these effects result from complex formation of ligand with Co (II), Ni (II), Cu (II) and Bi (V). Metal coordination to novel ligand was studied by various spectroscopic techniques. The crystal system, lattice parameters, unit cell, particle size and volume were determined by XRPD. The crystallographic data of complex (1) are: triclinic, space group P1, a(Å) =15.621, b(Å) =14.119, c (Å) =23.491, V(Å^3) =1112.00, α^o = 48.183, β^o =37.56,γ^o = 30.72 and for complex (4): crystal system, Triclinic, space group, P-1, a (Å) =8.290549, b(Å) =9.619387, c(Å) =16.12853, α^o = 63.75208, β^o =53.3017, γ^o =62.28692,V(Å^3 } =1611.49. The molecular structures of the complexes were optimized by and calculations which indicated a square planar arrangement of ligand around the Co(II) ions.

Keywords: Aminoglycoside, Gentamicin, amoxicilline, antibiotics, Spectra, Metal binding, Molecular modeling.

INTRODUCTION

Gentamicin and amoxicillin are both antibiotics. Gentamicin is an aminoglycoside antibiotic, used to treat many types of bacterial infections, particularly those caused by Gram-negative bacteria. However, gentamicin is not used for Neisseria gonorrhoeae, Neisseria meningitidis or Legionella pneumophila bacterial infections (because of the risk of the patient going into shock from lipid A endotoxin found in certain gram negative organisms). It is synthesized by icromonospora, a genus of Gram-positive bacteria widely present in the environment (water and soil). To highlight their specific biological origins, gentamicin and other related antibiotics produced by this genus (verdamicin, mutamicin, sisomicin, netilmicin, and retymicin) have generally their spellings ending in ~micin and not in ~mycin. Gentamicin is a bactericidal antibiotic that works by binding the 30S subunit of the bacterial ribosome, interrupting protein synthesis[1-11]. Like all aminoglycosides, when gentamicin is given orally, it is not systemically active. This is because it is not absorbed to any appreciable extent from the small intestine. It appears to be completely eliminated unchanged in the urine. Urine must be collected for many days to recover all of a given dose because the drug binds avidly to certain tissues. It is administered intravenously, intramuscularly or topically to treat infections. coli has shown some resistance to gentamicin, despite being Gram-negative[12-17].

Gentamicin is one of the few heat-stable antibiotics that remain active even after autoclaving, which makes it particularly useful in the preparation of certain microbiological growth media. Treatment of susceptible bacterial infections, normally Gram-negative bacteria including Pseudomonas, Proteus, Serratia, and Gram-positive Staphylococcus[13,14].

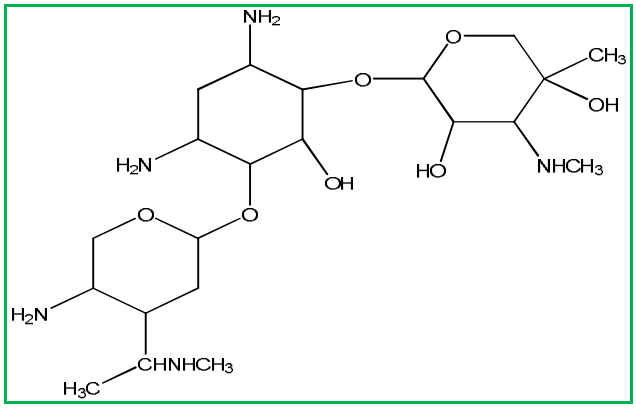

Figure 1: Gentamicin C

Amoxicillin is a member of penicillin's group which are a very important class of β-lactamic antibiotics used in therapy because of their specific toxicity towards bacteria. From a coordination chemistry perspective it has been demonstrated that all the β-lactamic antibiotics possess a number of potential donor sites and they are known to interact effectively with several metal ions and organometallic moieties, originating complexes[16,17]. Atoms involved in coordination and the structure of these complexes depend on several factors including reaction medium, pH, conformational equilibrium occurring in solution state and nature of the side chain bonded at C of the β-lactamic ring.

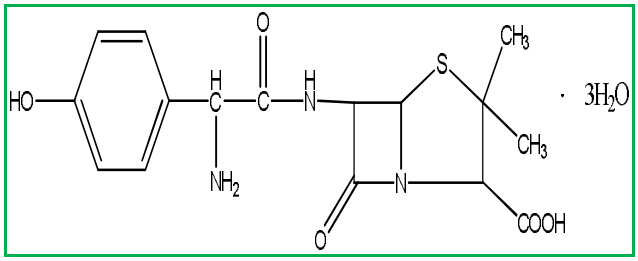

Figure 2: Amoxicillin Trihydrate

Cobalt, nickel, copper and its compounds have been shown antibacterial sensitivity[18] Bismuth and its compounds have medicinal applications[19] in treatment of a variety of gastrointestinal disorders, including gastric and duodenal ulcers, dyspepsia, diarrhea and colitis. Short-life α-emitter bismuth isotopes (^{212}Bi, ^{213}Bi) have been used as radio targets for cancer therapy. Bismuth is known for the synthesis of renal metallothionein, MT, forming a very strong complex [Bi_2MT]. Pretreatment with bismuth complexes prevent the toxic side effects of the anticancer drug, cisplatin, without compromising its antitumor activity[20]. It binds preferentially to the human serum transferring.[21] Bismuth compounds have become attractive candidates for use as reagents in organic synthesis,[22] in semiconductors, cosmetic preparations, alloys and metallurgical additives and in recycling of uranium nuclear fuels[23]. The field of organometallic chemistry, particularly the synthesis of bismuth-organic frameworks, has received much attention due to their various applications in bioinorganic and coordination chemistry[24]. Bismuth-organic frameworks are a growing class of organometallic compounds, which demonstrate a wide range of structures due to their different molecular topologies, synthesized by varying the set of donor atoms in the organic ligand. The formation of such frameworks depend significantly on the dimension of the internal cavity, rigidity of the ligands, nature of electronegative atoms present in the ring and complexing properties of the anion involved in the coordination. Their stability also depends upon a number of factors, including the number and types of donor atoms present in the ligand and their relative positions within the ligand skeleton. The organic framework is a new ligand, which has various applications in industry and medicine[25]. The coordination chemistry of bismuth is disproportionately sparse when compared with earlier reports[26]. The coordination abilities of nitrogen and oxygen donor atoms are used in the present study and described with spectroscopic characterization techniques. The bond formation between bismuth and the asymmetric ligand is detected, studied and explored by various spectroscopic techniques, molecular modeling and XRPD studies. The antibacterial sensitivity of the complexes also carried out by different methods. The ligand used in present work has been synthesized and it was characterized by elemental analysis, infrared spectra, ^{1}HNMR spectra and mass spectra. Satisfactory results were obtained shown in figure 3.

Experimental details

All chemicals were obtained from Aldrich Chemical Co, USA and used as received.

Physical measurements

Elemental (C, H and N) analyses were carried out on a Carlo-Erba 1106 Elemental Analyzer. IR spectra were recorded on a PerkinElmer 137 instrument as KBr pellets. Electronic spectrum of the solid complex was recorded in DMSO solution on a Shimadzu UV mini-1240 spectrophotometer. ^{1}H NMR spectra of the ligand and its complex were recorded on Bruker Avance 300 spectrophotometer at 100 kHz modulation and higher frequency. Electron impact mass spectra were recorded on JEOL, JMS, and DX-303 mass spectrometer.

XRD measurement and molecular modeling

The XRD powder patterns of the all complexes was recorded on a vertical type Philips 1130/00 diffractometer, operated at 40 kV and 50 mA using the monochromatized Cu-Kα line at wavelength 1.54056 A˚ as the radiation source. The sample was scanned between 5^o to 70^o at 25^{o}C. The crystallographic data was analyzed by using the CRYSFIRE-2000 powder indexing software package and the space group was found by the GSAS program[28]. The Debye – Scherer relation in conjunction with estimation of 100% peak width was used to estimate the particle size. The density was determined by using Archimedes method. Molecular modeling was performed by the latest version of the software.

Preparation of Bi(V) solution

Sodium bismuthate was dissolved in 1:1 $HClO_4$ and 0.1 M HCl. After filtration, the transparent filtrate was obtained and further used as Bi (V) source for the formation of complex.

Preparation of ligand solution

Equimolar amounts of 2-(4,6-diamino-3-(5-amino-4-((methyl amino)ethyl)tetrahydro-2H-pyran-2-yloxy)-2-hydroxycyclohexyloxy)-5-methyl-4-(methylamino) tetra hydro-2H-pyran-3,5-diol(gentamicin-C) and 6-(2-amino-2-(4-hydroxyphenyl)acetamido)-3,3-dimethyl-7-oxo-4-thia-1-azabicyclo[3.2.0]heptane-2-carboxylicacid trihydrate (Amoxicillin) were dissolved in CH_3OH and reflux on water bath for 6h. After filtration, a transparent filtrate was obtained. The filtrate on slow evaporation at room temperature forms fine crystals. This was recrystalised in methanolic solution and washed with hot methanol and again left slow evaporation a beautiful crystal was obtained. Ligand is soluble in common polar solvents. Reaction:

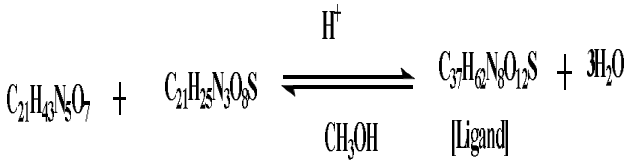

Light yellow crystal-yield: 85%;

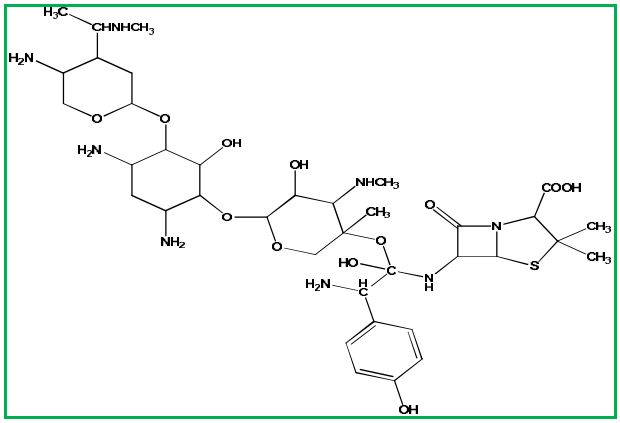

Figure 3: Molecular structure of 6-((1S,2S)-2-amino-1-(6- (4,6-diamino-3- (5-amino-4- (1-(methylamino) ethyl)tetrahydro -2H- pyran- 2- yloxy)-2hydroxy cyclohexyloxy) -5- hydroxyl -3-methyl-4- (methylamino) tetrahydro-2H-pyran-3-yloxy)- 1- hydroxy-2- (4-

hydroxyphenyl) ethylamino) -3, 3- dimethyl-7 -oxo-4-thia-1-azabicyclo [3.2.0] heptane-2-carboxylic acid (L) Chemical Formula: $C_{37}H_{62}N_8O_{12}S$ (A New ligand).

General method for the synthesis of complexes

A hot solution (1mmol, 20mL) of, of 6-((1S,2S)-2-amino-1-(6-(4,6-diamino-3-(5-amino-4-(1-(methylamino) ethyl) tetrahydro-2H-pyran-2-yloxy)-2-5-hydroxy-3 ethyl-4-(methylamino)tetrahydro-2H-pyran-3-yloxy)-1-hydroxy-2- (4-hydroxyphenyl) hylamino)-3,3-dimethyl-7-oxo-4-thia-1-azabicyclo[3.2.0]heptane-2-carboxylic acid(L) (1 mmol) in 80% CH_3OH (20 mL) was added to another CH_3OH solution of (20 mL) corresponding metal salt (1 m mol). Both solutions were mixed in 100 ml round bottom flask and refluxed for 6h at room temperature. The precipitate was filtered and washed with 50% methanol and dried in vacuum. This process of complex 4 was carried out as usual.

Antibacterial sensitivity assay

Antibacterial sensitivity assay was performed using novel legand (L) and its metal complexes complex1, complex2, complex3 and complex4 on *Agrobacterium sp* BN-2A. Various concentrations (0, 25, 50, 100, 150 and 200 µg/mL) were made and filter sterilized with 45mm sterile filter paper. Antibiotic discs were prepared with Watt's man filter paper to cut by paper punch machine. All paper discs were autoclaved and soaked with filter sterilized antibiotic solutions of different concentrations separately in sterile condition then excess water of solution was dried in oven. Now, antibiotic discs of different concentrations were ready to use. 100 µL aliquot of overnight nutrient broth grown culture (*Agrobacterium sp* BN-2A) was spread over Nutrient agar (NA) solid Petri plate and antibiotic discs were kept gently on the surface. The Petri plates were incubated in BOD incubator at 37^0C for growth. Inhibition zone was visualized around antibiotics disc after overnight growth. The diameter of the zone of inhibition and antibiotic discs were recorded. Bacterial inhibition index (BII) was calculated using formula written below:

$$\text{Bacterial Inhibition Index (BII)} = \frac{\text{Diameter of inhibition zone} - \text{Diameter of antibiotic disc}}{\text{Diameter of antibiotic disc}}$$

The experiment was performed in triplicate and repeated three times. Average of all readings and standard deviations were calculated. Statistical calculations (t-test) were done and P-value was recorded. P value ($p \leq 0.005$) showed the significant data.

RESULTS AND DISCUSSION

Satisfactory results of elemental analysis (Table 1) and spectral studies revealed that the complexes were of good purity. Various attempts to obtain the single crystals have so far been unsuccessful. X-ray diffraction studies indicate crystalline nature of the metal complexes. The complexes were soluble in polar solvents.

Table 1: Color, reaction yield and elemental analysis of complexes

Compound	Empirical formula	Color	Yield (%)	Analysis: found (calculated) (%) C	H	N	S	M
Ligand(L)	$C_{37}H_{62}N_8O_{12}S$ 842.42	Light yellow	85	52.74 (52.72)	7.45 (7.41)	31 (13.29)	3.81 (3.80)	
[Co(L)(2H_2O)]	$C_{37}H_{64}CoN_8O_{14}S$ 935.95	Pink	80	47.71 (47.78)	6.85 (6.89)	11.97 (11.97)	3.45 (3.43)	6.31 (6.30)
[Ni(L)H_2O] H_2O	$C_{37}H_{64}N_8NiO_{14}S$ 935.71	Green	81	47.45 (47.49)	6.85 (6.89)	11.95 (11.98)	3.45 (3.43)	6.28 (6.27)
[Cu(L)H_2O]	$C_{37}H_{64}CuN_8O_{14}S$ 940.56	blue	80	47.26 (47.25)	6.85 (6.86)	11.92 (11.91)	3.45 (3.41)	6.78 (6.76)
[Bi(L)OClO4]	$C_{37}H_{60}BiC_{l3}N_8O_{24}S$ 1348.32	White	75	32.97 (32.96)	4.45 (4.49)	8.35 (8.31)	2.36 (2.38)	15.52 (15.50)

L: Ligand

Vibrational spectra

Ligand molecule exhibits absorptions 1050, 1750, 2934cm^{-1}. These bands are very metal complexes indicating non – involvement of the oxygen atoms of hydroxyl group in coordination with the metal ions[27]. The stretching frequencies of ligand hydroxyl and give bands at 3368 and 3434 cm^{-1} with a shoulder at about 3550 cm^{-1}. These bands appear in the complexes as strong band absorption in the region 3420 - 3445 cm^{-1}. These bands appear for the new complex at the same wave number, ruling out the participation of hydroxyl oxygen in the coordination. These results confirm that complexation occurred and suggest that the oxygen of the hydroxyl group is involved in the coordination sphere[28]. The vibrational bands due to rocking and wagging modes of water and metal – oxygen stretching modes are observed in the 800 – 350 cm^{-1} region for all the complexes may be attributed to coordinated water[29]. This can be confirmed with the help of thermo grams. A new band in the 615 – 300cm^{-1} regions in the spectra of the complexes is assignable to ν (M - O) and ν (M-ClO_4) appeared at 925, 931, and 932 in complex 4.

^{1}H NMR spectra

The ^{1}H NMR spectra in a DMSO–d_6 solvent of the ligand and Co(II)-ligand complex show well resolved signals. The N-H protons of amine would have undergone very rapid exchange with the solvent appear as quite broad ragged doublet around 2.0ppm. In all complexes, peaks in the range 1.20 – 1.60 ppm are from coordinated water. The various assignments of ^{1}H NMR of the ligand and metal (II) complexes are summarized in table 3. Chemical shift are in ppm from TMS & multiplicity in parentheses (bd: broad; d: doublet; m: multiplet)

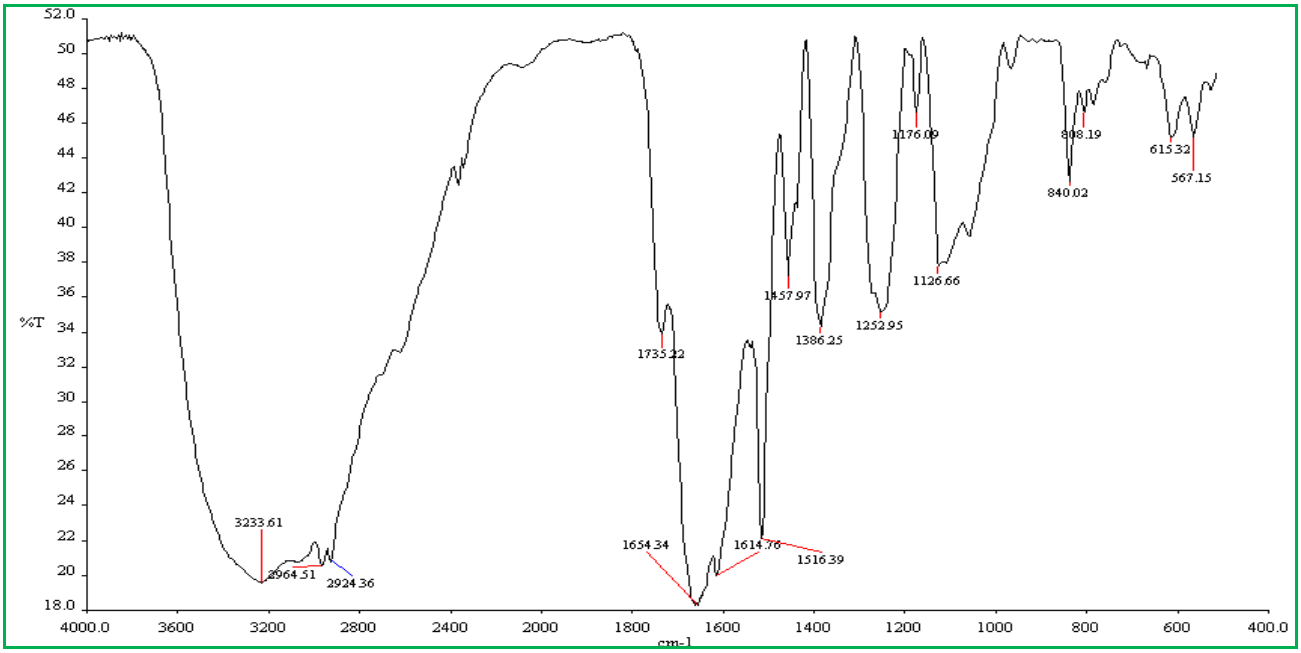

Figure 4: FT-IR spectra of new ligand

Table 2: IR spectral data (cm^{-1}) of the metal complexes

Frequency	ν_{N-H}	OH	OH	NH_2	NH_2	M - O	M-ClO_4
[Co(L)H_2O]	3434(s,b)	1636(m)	1515(s)	1220(m)	695(s)	405(m)	
[Ni(L)H_2O]	3429(s,b)	1639(m)	1510(s)	1210(m)	690(s)	465(s)	
[Cu(L)H_2O]	3445(s,b)	1634(m)	1508(m)	1219(w)	692(s)	372(m)	
[Bi(L)H_2O]	3421(s,b)	1626(m)	1489(s)	1215(w)	695(s)	365(s)	925,931,962

Table 3: ^{1}HNMR data of free ligands and their complexes

Compounds	δ (ppm)
Ligand	[3.35(s)1H,OH],16.77(s)1H,OH,16.77(s),1H,OH,3.65(m),5H,OH,2.0(s)1H,NH,7.16(s)!H,NH_2 3.83(m)1H,CH,8.19(d)1H,CH(Ar),7.00(s)1H,CH(Ar),7.62(m)1H,CH(Ar),6.78(s)1H,CH(Ar),2.52---3.98(m)4H,(m)CH,3.98—4.73(d),2H,CH,1.35(s) 3H,Ch,1.06(s)6H,CH_3].
Complex 1	[3.35(s)1H,OH], 16.77(s),1H,OH,3.65(m),5H,OH,2.0(s)1H,NH,7.16(s)!H,NH_2 3.83(m)1H,CH,8.19(d)1H,CH(Ar),7.00(s)1H,CH(Ar),7.62(m)1H,CH(Ar),6.78(s)1H,CH(Ar),2.52---3.98(m)4H,(m)CH,3.98—4.73(d),2H,CH,1.35(s) 3H,Ch,1.06(s)6H,CH_3].
Complex2	[16.771H(s)Ar-OH],3.65,8H(m),OH],8.562H(s),NH_2],2.06H(s) ,NH],[3.76,5H(m)CH]3.56,7H(m),CH_3]
Complex3	[3.65(m),5H,OH],[3.58(s),4H,OH,][2.0(s)4H,NH],8.56(s)1H,NH_2,]3.514.24(m)4H,CH],[5.03(d)1H,CH],3.76—3.81(m),6H CH],8.19(s)1H ,CH] 8.89(m)1HCH(Ar)],[7.62(s)1H,CH],[9.72(s)1H,CHO],4.73(m)1HCH,3.79 2H,CH2,3.17(m)6H,CH_3,1.18(m) 3H,CH_3].
Complex4	[5.35,1H(s),Ar-OH],[11.01H(s),COOH],5.11,2H(d),NH_2,],[8.03,1H(s),NH],3.00-7.10,8H(M0,CH],[1.35,5H(m),CH_3].

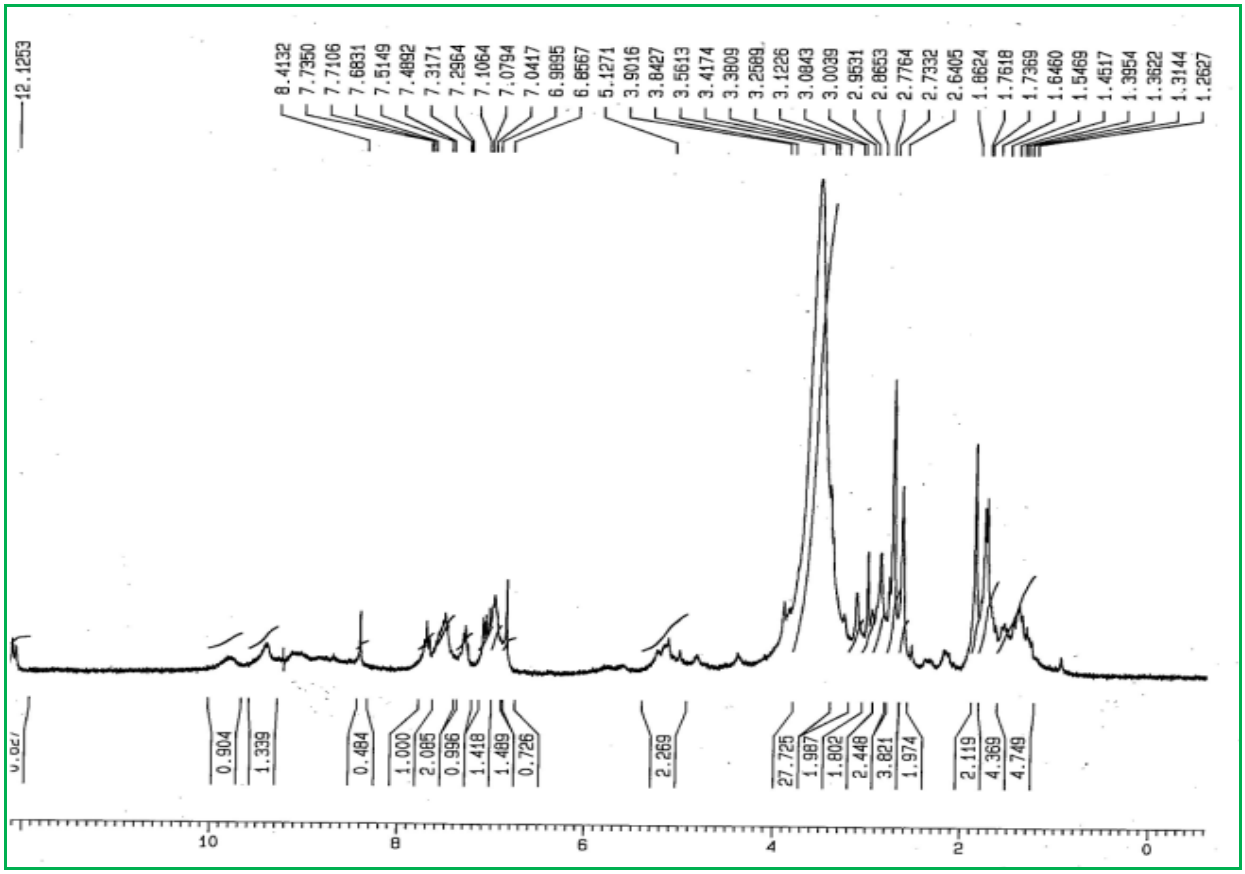

Figure 5: ^{1}H NMR spectra of the ligand.

Electronic spectra and magnetic susceptibility

The electronic spectra of the ligands and its metal complexes have been studied in the range 190 – 800 nm. The shoulder band observed at 275nm in water solvent in ligands may be assigned to n → n * transition within the OH group of the hydroxyl moiety in the free ligands. This band is disappeared in all the complexes, revealing the involvement of the OH of hydroxyl group oxygen in chelate formation. The band observed at 296nm in ligand may be assigned to π → π* transition of the oxygen of hydroxyl group of ligand. In the cobalt complex, the absorption band in the visible region 508-565 nm & 470-430 nm assignable to $^{2}A_{1g} \rightarrow {}^{2}B_{2g}$(P) & $^{2}B_{2g} \rightarrow {}^{4}A_{2g}$(P) transition, suggesting square planar geometry of the cobalt complex, whereas in the nickel complex, absorption bands in the visible region 729 – 657nm and 582 –565 nm may be assigned to the $^{1}A_{1g} \rightarrow {}^{1}A_{2g}$ and $^{1}A_{1g} \rightarrow {}^{1}B_{1g}$ transitions respectively, which are consistent with a square planar stereochemistry with the nickel (II) ions[30]. The magnetic moment of the cobalt complex is 2.7 BM at room temperature. The reason for the departure from the spin only value lies partly in the existence of the second order Zeeman Effect between the ground and higher ligand field terms[31]. However, it lies mainly in fact that in the presence of spin orbit coupling the quenching effect of the ligand field cannot be complete. The electronic spectrum of copper complex 765nm due to d-d transition and was assigned to $^{3}B_{1g} \rightarrow {}^{2}E_{2g}$ suggesting an octahedral geometry around Cu (II) ion[32]. In the case of Bi (V) ions it had shown diamagnetic in nature. The geometry about the bismuth atoms in the solid state is trigonal bipyramidal in complex 4.

Kinetics of thermal decomposition

Recently, there has been increasing interest in determining the rate dependent parameters of solid-state non-isothermal decomposition reactions by analysis of TG curves. Thermogravimetric (TG) and differential thermo gravimetric (DTA) analyses were carried out for different metal–legand complexes in ambient conditions. The thermogravimetric analysis revealed that the complexes of cobalt & nickel loses mass between 65°C and 140°C, corresponding to nearly 13 % of the total mass, followed by considerable decomposition up to 600°C, which corresponds to the decomposition of the ligand molecule leaving metal oxide (CoO & NiO, respectively) as residue. The complexes of copper & bismuth decomposes nearly 9% of the total mass up to temperature 170°C, followed by considerable decomposition of the ligand molecule up to 650°C, leaving metal oxide (CuO and Bi_2O_5 respectively) as residue. On the basis of thermal decomposition, the kinetic analysis parameters such as activation energy (E*), enthalpy of activation (ΔH*), entropy of activation (ΔS*), free energy change of decomposition (ΔG*) were evaluated graphically by employing the Coats – Redfern relation[29]

$$\text{Log } [-\text{Log } (1- \alpha) /T^2] = \log [AR/ \theta E^*(1-2RT/E^*)]-E^*/2.303RT$$

Where α is the mass loss up to the temperature T, R is the gas constant, E*is the activation energy in J mole^{-1}, θ is the linear heating rate and the term (1-2RT/E*) ≅ 1.A

straight line plot of left hand side of the equation (1) against 1/T gives the value of E* while its intercept corresponds to A (Arrhenius constant). The Coats and Redfern linearization plots, confirms the first order kinetics for the decomposition process. The calculated values of thermodynamic activation parameters for the decomposition steps of the metal complexes are reported in Table 4. According to the kinetic data obtained from the TG curves, the activation energy relates the thermal stability of the metal complexes. Among metal complexes, activation energy increases as complex III ~ complex II < complex IV < complex I, same trends happens with thermal stability of metal complexes. All the complexes have negative entropy, which indicates that the complexes are formed spontaneously. The negative value of entropy also indicates a more ordered activated state that may be possible through the chemisorptions of oxygen and other decomposition products. The negative values of the entropies of activation are compensated by the values of the enthalpies of activation, leading to almost the same values for the free energy of activation.

Table 4: Thermodynamic activation parameters of the metal complexes

Complex	Order/n	Steps	E*/Jmo^{1}	A/sec^{-1}	ΔS*/JK^{-1}mol^{-1}	ΔH*/Jo^{1}	ΔG*/ Jmol^{-1}	k×10^{3m-1}
[Co(L)2H_2O]	1	I II	33.145 68.29	1.045×10^{5} 0.564×10^{5}	-107.21 -11.206	45.26 65.231	42.19 91.81	1.02 1.79
[Ni(L)2H_2O]	1	I II	31.01 68.26	1.56×10^{5} 0.564×10^{5}	-105.096 -138.37	35.24 65.321	38.55 11.89	1.53 7.05
[Cu(L)2H_2O]	1	I II	33.526 46.79	1.25×10^{4} 0.425×10^{4}	-99.68 -107.21	45.256 65.24	42.19 91.81	1.02 1.79
[Bi(L)3ClO_4]	1	I II	40.163 72.98	1.735×10^{6} 0.325×10^{6}	-41.91 -117.24	34.01 34.324	39.97 102.67	3.22 1.72

Table 5: Crystallographic data for complexes

Compounds	Complex 1	Complex 2	Complex 3	Complex 4
Formula	$C_{37}H_{64}CoN_8O_{14}S$	$C_{37}H_{64}N_8NiO_{14}S$	$C_{37}H_{64}CuN_8O_{14}S$	$C_{37}H_{60}BiCl_3N_8O_{24}S$
FW	935.95	935.71	940.56	1348.32
Temp (K)	293	293	293	293
Wavelength	1.54056	1.54056	1.54056	1.54056
Crystal System	Triclinic	Orthorhombic	Monoclinic	Triclinic
Space group	P-1	P 21/M	P 2/M	P 1
Unit cell dimension				
A(Å)	15.621	19.278	15.835	9.172
B(Å)	14.119	15.531	7.8728	12.6752
C(Å)	23.491	6.007	11.5068	13.6812
α^0	48.183	90.0000	90.00	126.215
β^0	37.56	90.000	129.7128	40.552
γ^0	30.72	90.000	90.00	145.475
Volume (Å ^{3})	1611.49	1798.324	1103.5	583.48
θ range (0)	19.0-70.0	7.0-30.0	9.0-78.0	11.00-70.00
Limiting indices	0 ≤ h ≤ 8 0 ≤ k ≤ 5 0 ≤ l ≤ 2	0≤ h ≤ 7 0 ≤ k ≤ 2 0 ≤ l ≤ 2	-7≤ h ≤ 5 0 ≤ k ≤ 5 0 ≤ l ≤ 6	-1≤ h ≤ 3 -5 ≤ k ≤ 3 0 ≤ l ≤ 6
Particle size(nm)	49.123	50.341	45.324	60.412
Intensity (%)	7.2–100	5.9–100	5.3-100	6.1-100
Avs.Eps.	0.0000106	0.000131	0.00006123	0.0000442
Density	1.921	1.199	1.412	1.765
Z	2	1	1	1

TOF–MS spectra

Mass spectrometry has been successfully used to investigate molecular species $[MH]^+$ in solution . The molecular ion peaks of the ligands and complexes have been used to confirm the proposed formula. The mass spectrum of ligand with different fragmentations: m/z: 842.42 (100.0%), 843.42 (43.8%), 844.43 (10.7%), 844.42 (6.1%), 845.42 (2.2%), 845.43 (2.2%), 843.43 (1.2%) The pattern of the mass spectrum gives an impression of the successive degradation of the target compound with the series of peaks corresponding to the various fragments. Their intensity gives an idea of stability of fragments. The ligand starts degradation and finally forms $[C_{14}H_{30}N_4O_4]$ e,317/318(100 % m/z values. In the TOF–mass spectra of metal complexes initial fragmentation pattern is again similar (loss of two water molecules), a mononuclear nature for these complexes $[M(L)]^+$ can be deduced. The last two fragments appears in nearly all the complexes at positions (m/z values) 165(100% complex 1, 100 % complex 2, 100 % complex 3 and 57 % complex(4) and 224/225/227 (10 % complex I, 50% complex 2 and 100 % complex IV) corresponds to $[C_5H_{24}N_2O_3]^+$ and $[C_9H_{12}NO_3S]^+$ respectively, which could be the result of degradation & demetallation of the complexes and the mass spectrum of complex 4 $[Bi(V)(L)OClO_3]$ gives molecular masses with different fragmentations: m/z: 1348.23 (100.0%), 1346.23 (98.0%), 1349.23 (44.9%), 1350.23 (44.1%), 1347.23 (42.9%), 1351.23 (14.9%), 1348.24 (13.1%), 1352.23 (5.1%), 1352.22 (4.6%), 1350.22 (4.3%), 1349.24 (3.2%), 1351.24 (3.1%), 1353.23 (2.3%), 1347.24 (1.6%), 1350.24 (1.3%), 1351.22 (1.3%)

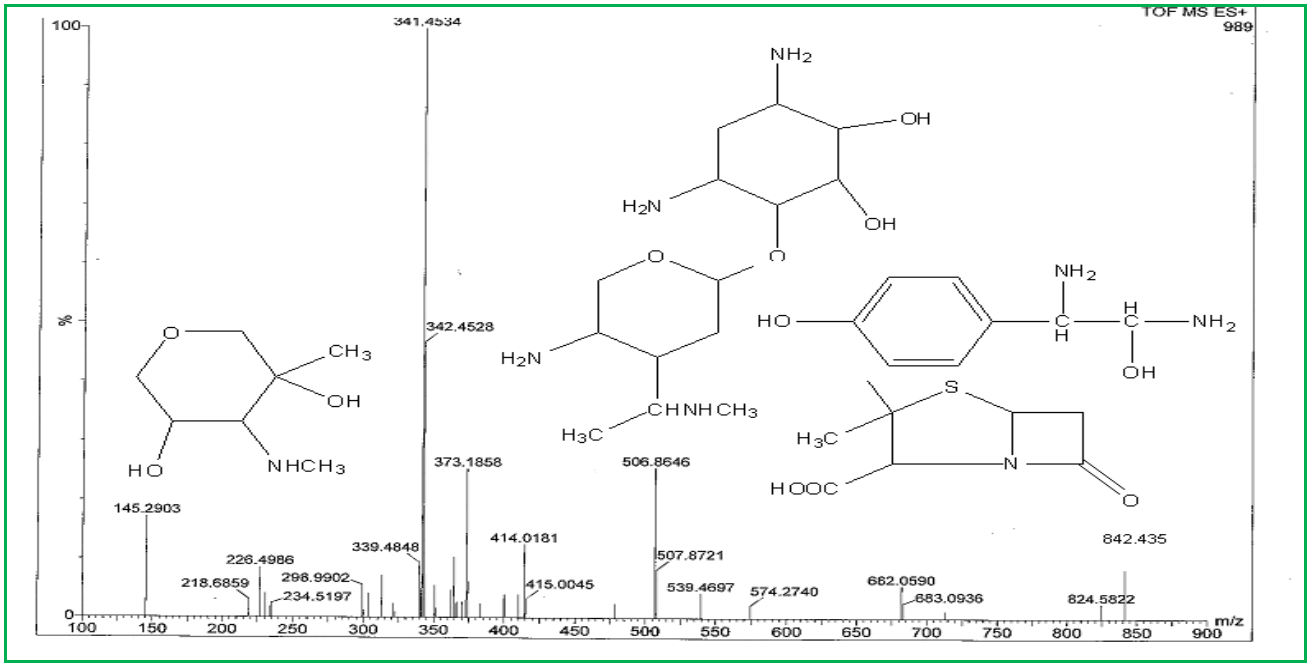

Figure 6: TOF-Mass spectra of ligand

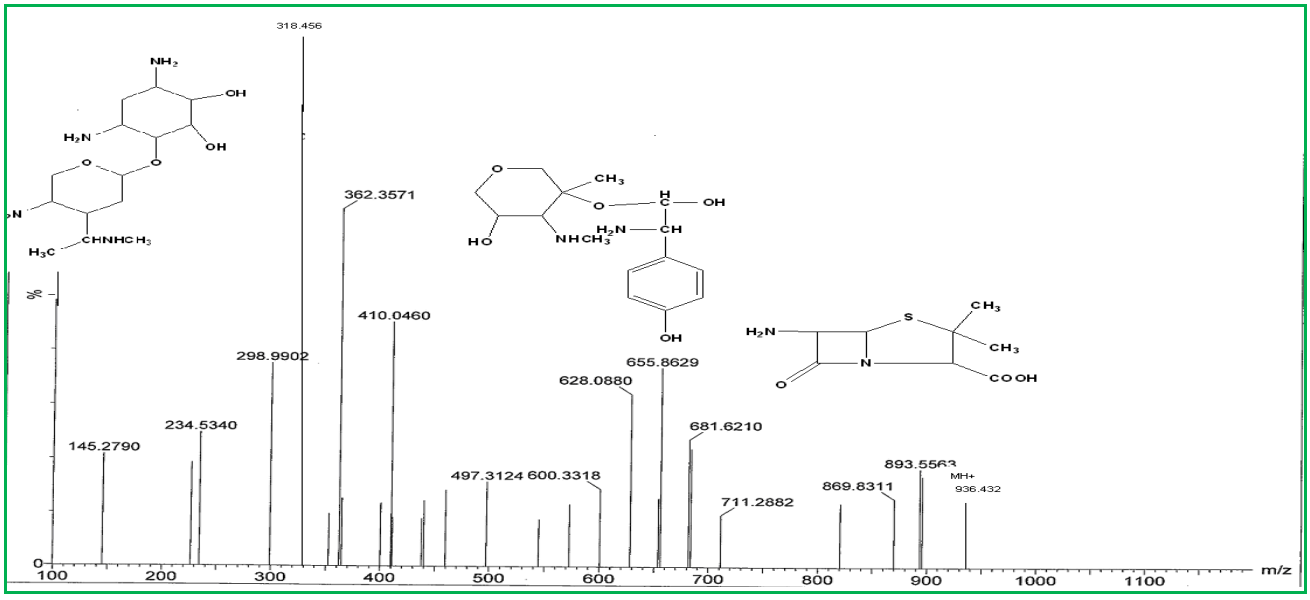

Figure 7: TOF- Mass spectra of complex 1

X-ray powder diffraction study

X-ray powder diffraction patterns of all complexes were recorded between 9 and 80(2θ). The value of (2 θ), interplanar spacing d (A) and the relative intensities (I/I_0) of the compounds under study with help of CRYSFIRE - 2000 [30] were recorded in table 5.

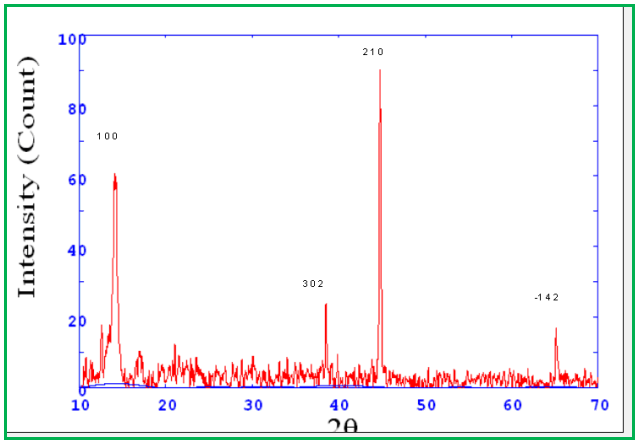

Figure 8: XRPD spectra of ligand

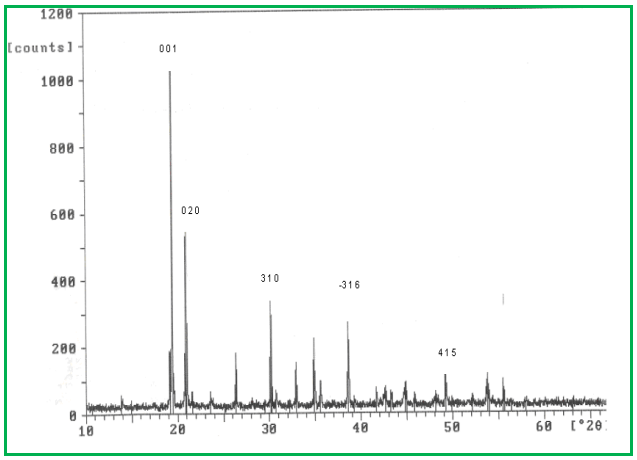

Figure 9: XRPD spectra of complex 2

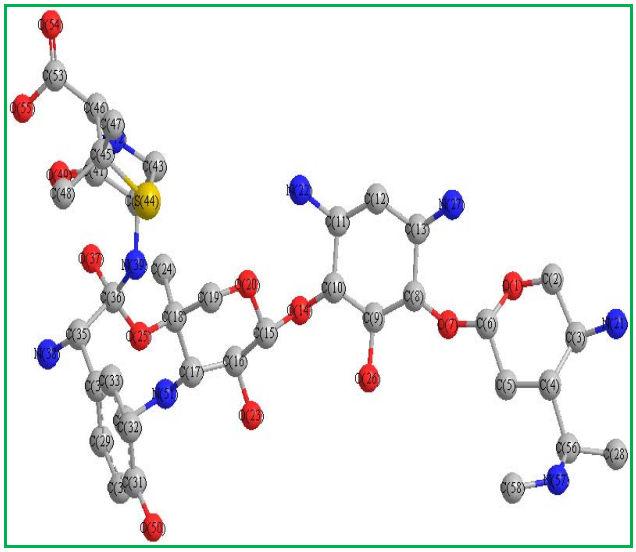

Figure 10: Optimised structure ligand. Hydrogen atoms have been omitted for clarity.

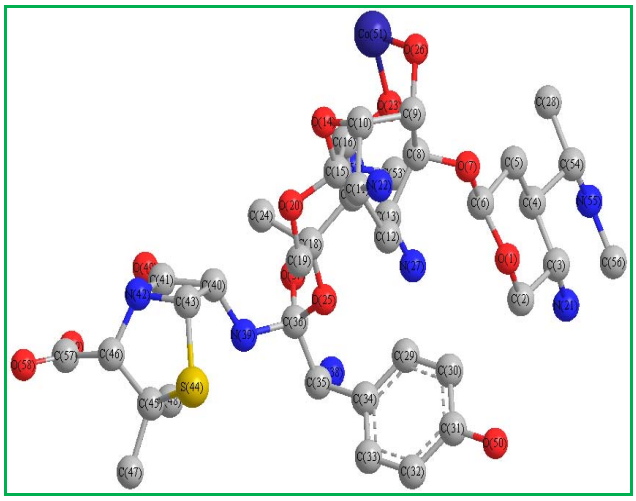

Figure 11: Optimised structure of complex 1.Hydrogen atoms have been omitted for clarity.

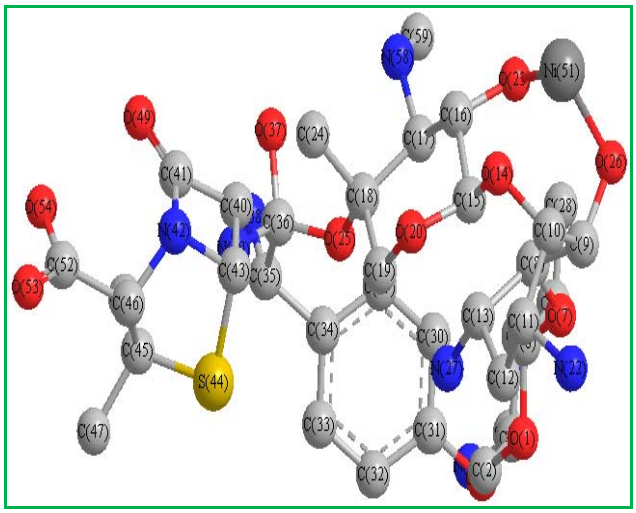

Figure 12: Optimised structure of complex 2.Hydrogen atoms have been omitted for clarity

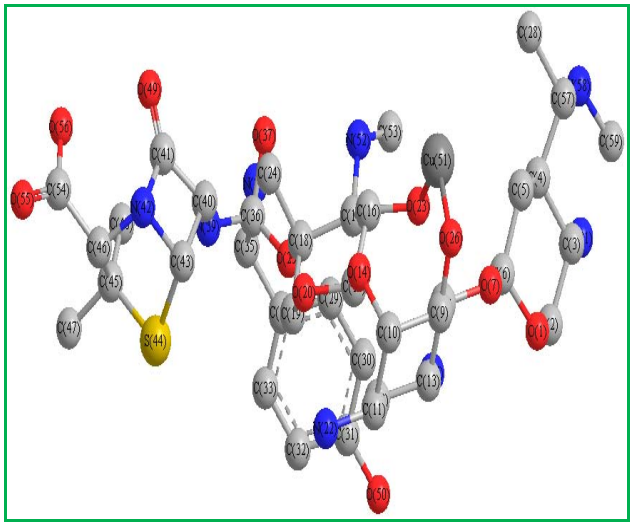

Figure 13: Optimised structure of complex structure of complex 3 with Hydrogen atoms have been omitted for clarity

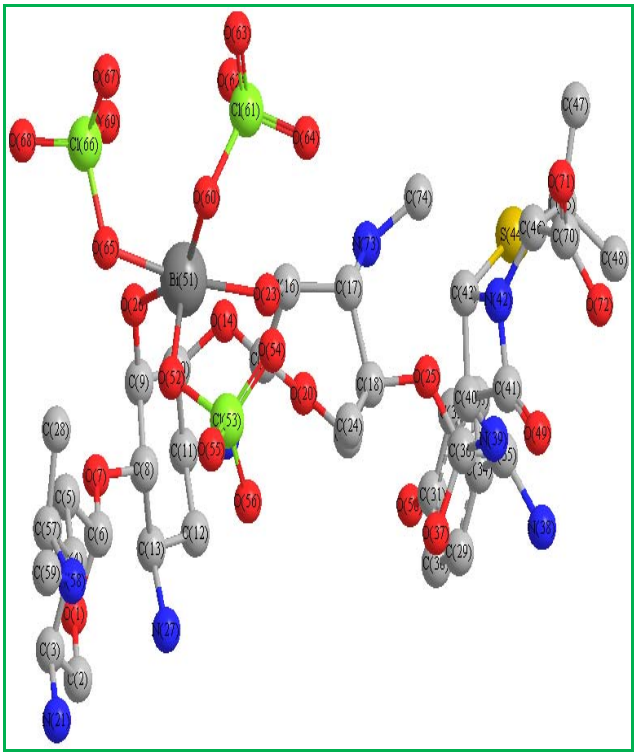

Figure 14: Optimised structure of complex 4.Hydrogen atoms have been omitted for clarity

Table 6: Data for selected bond lengths and bond angles of complexes

Bond length Å		Bond angle°	
Complex1		**Complex(1)**	
Ni(51)-O(53)	1.7744	O(53)-Co(51)-O(52)	154.7863
Ni(51)-O(52)	1.7747	O(53)-Co(51)-O(23)	151.3057
O(23)-Ni(51)	1.7705	O(53)-Co(51)-O(26)	115.2137
O(26)-Ni(51)	1.7732	O(52)-Co(51)-O(23)	3.4806
		O(52)-Co(51)-O(26)	90.0000
		O(23)-Co(51)-O(26)	93.4806
Complex2		**Complex(2)**	
Co(51)-O(53)	1.8000	O(53)-Ni(51)-O(52)	105.0667
Co(51)-O(52)	1.8000	O(53)-Ni(51)-O(23)	112.2802
O(23)-Co(51)	1.7947	O(53)-Ni(51)-O(26)	108.8740
O(26)-Co(51)	1.8000	O(52)-Ni(51)-O(23)	108.0728
		O(52)-Ni(51)-O(26)	107.8576
		O(23)-Ni(51)-O(26)	114.1955
Complex3		**Complex3**	
Cu(51)-O(53)	1.8100	O(53)-Cu(51)-O(52)	108.9672
Cu(51)-O(52)	1.8100	O(53)-Cu(51)-O(23)	109.9496
O(23)-Cu(51)	1.8098	O(53)-Cu(51)-O(26)	109.9496
O(26)-Cu(51)	1.8100	O(52)-Cu(51)-O(23)	109.6505
		O(52)-Cu(51)-O(26)	109.6505
		O(23)-Cu(51)-O(26)	108.6627
Complex4		**Complex4**	
Bi(50)-O(56)	2.1027	Bi(50)-O(61)-Cl(62)	113.9611
Bi(50)-O(51)	2.1028	Bi(50)-O(56)-Cl(57)	112.6214
Bi(50)-O(61)	2.1043	Bi(50)-O(51)-Cl(52)	117.7915
O(49)-Bi(50)	2.1060	O(56)-Bi(50)-O(51)	98.2023
C(18)-Bi(50)	2.2405	O(56)-Bi(50)-O(61)	140.4648
		O(56)-Bi(50)-O(49)	80.1912
		O(56)-Bi(50)-C(18)	90.7443
		O(51)-Bi(50)-O(61)	85.5717
		O(51)-Bi(50)-O(49)	148.4270
		O(51)-Bi(50)-C(18)	98.1493
		O(61)-Bi(50)-O(49)	76.8385
		O(61)-Bi(50)-C(18)	127.8849
		O(49)-Bi(50)-C(18)	113.3646
		Bi(50)-O(49)-C(30)	112.4434
		Bi(50)-C(18)-C(24)	110.0389
		Bi(50)-C(18)-C(19)	103.8969
		Bi(50)-C(18)-C(17)	116.3045

Antimicrobial activity

The antibacterial sensitivity assay shows that there is increase of inhibitory potentials of antibiotic with novel by the formation of complex with metal[31-33]. The bacterial strain sensitive to ligand easily grow in the presence of 200 µg/mL of complex1 and complex2 where as the complex 3 was not effective up to 100 µg/mL and less effective on the concentration of 150 µg/mL and more. It can be seen in the table 1 and Fig.1 that only 25 µg/mL of ligand showed inhibitory effect on *Agrobacterium sp* BN-2A but the same strain is resistant to all concentrations of complex1 and complex 2 [The Bacterial Inhibition Index (BII) of ligand was highest (4.2 ± 0.245) at the concentration of 200 µg/mL and minimum inhibitory concentration (MIC) was 25 µg/mL where BII was 0.8 ± 0.047. The results show antibacterial activity increase in metal ions complexes may be due to effect metal ions on the normal cell process. The polarity of the metal ions is considerably reduced on chelation, which is mainly because of partially sharing of its positive charge with the donor groups and possibly delocalization of ring .Such chelation increases the liphophilic character of the metal complexes which probably breakdown of permeability barrier of the cells resulting in interference with normal cell process. The results shown in Table-7 (Fig. 14).

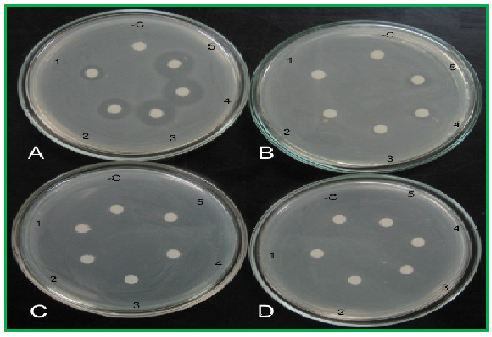

Figure 15: Antibacterial sensitivity assay of metal added antibiotics Streptomycin on *Agrobacterium sp* BN-2A.

A.nd; B, complex 1C, complex 2, complex 3(-C, 0.0 µg/mL; 1, 25 µg/mL; 2, 50 µg/mL; 3, 100 µg/mL; 4, 150 µg/mL; 5, 200 µg/mL concentration in ligand metal complexes of ligand

Table 7: Antibacterial sensitivity assay of ligand and its metal complexes on *Agrobacterium sp* BN-2A

Concentration (µg/mL)	BII of antibacterial novel ligand -metal complexes[#]				
	Ligand	Complex1	Complex 2	Complex 3	Complex 4
Control (-)	0 ± 0 (0)	0 ± 0 (0)	0 ± 0 (0)	0 ± 0 (0)	0 ± 0 (0)
25	0.8 ± 0.047 (0.2)	0.6 ± 0.05 (0.2)	0.5 ± 0.05 (0.2)	0.9 ± 0.01 (0.2)	0.842 ± 0.04 (0.2)
50	1.2±0.082 (0.002)	1.4 ± 0.01 (0.032)	1.3 ± 0.01 (0.032)	1.543±0.023(0.001)	2.43 ± 0.021 (0.032)
100	1.6±0.163 (0.003)	1.67 ± 0.0654 (0)	1.87 ± 0.0654 (0)	2.32± 0.01(0.021)	3.541 ± 0.02 (0.21)
150	2.2±0.245 (0.004)	3.7±0.032 (0.332)	3.6±0.032 (0.332)	3.2 ± 0.067 (0.01)	2.35± 0.021 (0.021)
200	4.2±0.245 (0.001)	1.50±0.082(0.169)	1.0±0.082 (0.169)	2.121±0.0654(0.001)	3.321± 0 .02(0.0012)

Values shown is the average ± standard deviation of three readings performed three times
[#]value in the parenthesis indicates p-value of the data based on t-test ($p \leq 0.005$).

CONCLUSION

This asymmetric ligand has several potential N/O atoms with different reactivity and electron density. The main interest was to understand the O/N bonding with different metal ions in the ligand system. The ligand moiety has different electro negativities, which influences the binding abilities of the ligand. Several spectroscopic techniques were used to understand the stabilities factors and coordination properties of mix ligands. The metal complex of ligand was synthesized. It was characterized by UV, IR, TG/DTA, TOF/MS and XRPD and structure were optimized with Rietveld refinement, Karl-Fischer titrametry and elemental analysis. By using these spectroscopic techniques, understandings of the stability and coordination ability of complexes were determined. The coordination behaviors of the anions are variable due to different coordinating sites of the ligand. It is quite understandable that the metal ions are five coordinate of complex4 with different atoms as well as anions. All the details about the studied complex are given in figures 2, 4 and 5. Observed data suggested five coordinate configurations around the metal in complex 4.. Transport of organic ligands into bacterial cells can be facilitated by the formation of metal complexes. The complex was found to possess metal to ligands ratio of 1:4. It has been observed that complexation between bismuth ions and ligands takes place above pH 7. The Solubility of complexes was found to be more than that of ligands. Agar diffusion method was used for antibacterial activity. The complexes were found to possess better activity (lesser MIC value) than that of ligand as well as bismuth (V) and ligands physical admixture. It was concluded that the complexes can be a better alternative to ligand as an antibacterial agent.

REFERENCES

1. Chauhan, H. P. S., Shaik, Nagulu Meera Singh. Synthetic, spectroscopic and antimicrobial studies of bis(dialkyldithi ocarbamato diorganodithio phosphate Bi(III) complexes, Applied Organometallic Chemistry, 19(10), (2005), 1132-1139.
2. Wojciechc Lesniak, Wesley R. Harris, Joslync Yudenfreundc Kravitz, Jochen Schacht, and Vincent L. Pecoraro, Solution Chemistry of Copper(II)-Gentamicin Complexes: Relevance to Metal-Related Aminoglycoside Toxicity, Inorg. Chem, 42 (5), (2003), 1420 -1429.
3. Nina Isoherranen, Stefan Soback, Determination of Gentamicins C_1, C_{1a}, and C_2 in Plasma and Urine by HPLC Clinica Chemistry 46, (2000), 837-842.
4. Nina Isoherranen and Stefan Sobac, Determination of gentamicin after trimethylsilyl imidazole and trifluoroacetic acid derivatization using gas chromatography and negative ion chemical ionization ion trap mass spectrometry, The analyst DOI, 10.1039/b0 03710i
5. Werner Winter, Ralph Deubner and Ulrike Holzgrabe Multivariate analysis of nuclear magnetic resonance data—characterization of critical drug substance quality of gentamicin sulfates Journal of Pharmaceutical and Biomedical Analysis, 38(2005), 833-839.
6. Eric M. Priuska , Kimber Clark-Baldwin b, Vincent L. Pecoraro b, Jochen Schacht, NMR studies of iron-gentamicin complexes and the implications for aminoglycoside toxicity, lnorganica Chimica Acta, 273, (1998), 85-91 .
7. Wojciech Szczepanik, Anna Czarny, Ewa Zaczynska, Malgorzata Je -zowska-Bojczuk, Preferences of kanamycin A towards copper(II). E.act of the resulting complexes on immunological mediators production y human leukocytes, Journal of Inorganic Biochemistry, 98, (2004), 245 –253.
8. Satoko Yoshzawa,Dominique fourmy and Joseph D.Puglisi,Structral origins of gentamicin antibiotic action,17,(1998).6437-6448.
9. Ma, Xiao-ling; Sun, Guang-ming; Dai, Yuan-yuan; Chen, Duo-yan; Lu, Huai-wei. Surveillance of antimicrobial resistance in staphylococcus aureus, Anhui Province Hospital, Hefei, Linchuang Shuxue Yu Jianyan 9(1), (2007), 18-20.
10. Huang, Ying; Xu, Yuan-hong; Wang, Zhong-xin; Feng, Ting. Detection of metallo -lactamase-producing imipenem-resistant Pseudomonas

aeruginosa and their antibiotic-resistance, Linchuang Shuxue Yu Jianyan 9, (2), (2007), 106-108.

11. Miao, Li,; Deng, Wan-jun, Progress in antibiotic prophylaxis of infective endocarditis, Guowai Yiyao Kangshengsu Fence 28(3), (2007), 124-129, 134.
12. Derome, Andrew; Hoischen, Christian; Bussiek, Malte; Grady, Ruth; Adamczyk, Malgorzata; Kedzierska, Barbara; Diekmann, Stephan; Barilla, Daniela; Hayes, Finbarr. Centromere anatomy in the multidrug-resistant pathogen Enterococcus faecium, Proceedings of the National Academy of Sciences of the United States of America, Early Edition, (Feb 1 2008), 1-6, 6 pp. Publisher: National Academy of Sciences.
13. Liu, Hai-ying; Chi, Fang-lu; Gao, Wen-yuan, Taurine attenuates aminoglycoside ototoxicity by inhibiting inducible nitric oxide syntheses expression in the cochlea, NeuroReport 19(1), (2008), 117-120.
14. Liu, Ding; Chen, Ping; Li, Yuhong; Yang, Cheng. Detection of aminoglycoside acetyltransferase genes in Acinetobacter baumannii by multiplex PCR, Di-San Junyi Daxue Xuebao 28(23), (2006). 2320-2322.
15. Holmes, Robert L.; Jorgensen, James H. Inhibitory activities of 11 antimicrobial agents and bactericidal activities of vancomycin and daptomycin against invasive methicillin-resistant Staphylococcus aureus isolates obtained from 1999 through 2006. Antimicrobial Agents and Chemotherapy 52(2), (2008), 757-760,
16. Castanheira, Mariana; Sader, Helio S.; Desphande, Lalitagauri M.; Fritsche, Thomas R.; Jones, Ronald N, Antimicrobial activities of tigecycline and other broad-spectrum antimicrobials tested against serine carbapenemase- and metallo- -lactamase-producing Enterobacteriaceae: Report from the SENTRY antimicrobial surveillance program. Antimicrobial Agents and Chemotherapy 52(2), (2008), 570-573,
17. Subramanian, Sreedhar; Roberts, Carol L.; Hart, C. Anthony; Martin, Helen M.; Edwards, Steve W.; Rhodes, Jonathan M.; Campbell, Barry J. Replication of colonic Crohn's disease mucosal Escherichia coli isolates within macrophages and their susceptibility to antibiotics. Antimicrobial Agents and Chemotherapy, 52(2) (2009)., 427-434.
18. Mindlin, S. Z. Soina, V. S. Petrova, M. A. Gorlenko, Zh. M., Isolation of antibiotic resistance bacterial strains from Eastern Siberia permafrost sediments, Russian Journal of Genetics, 44(1), (2008), 27-34.
19. P. Mishra, Bi(V) organic framework in an asymmetric system: Synthesis, spectroscopic, XRPD and molecular modeling DOI,10,1080/1024(2007) Online.
20. MacDonald, Iona; Staatz, Christine E.; Jelliffe, Roger W.; Thomson, Alison H. Evaluation and Comparison of Simple Multiple Model, Richer Data Multiple Model, and Sequential Interacting Multiple Model (IMM) Bayesian Analyses of Gentamicin and Vancomycin Data Collected From Patients Undergoing Cardiothoracic Surgery.Therapeutic Drug Monitoring 30(1), (2008). 67-74 ,
21. Li, Chun-yan; Yang, Qing urveillance of antimicrobial resistance and vancomycin resistance genes in Enterococcus species, Zhongguo Weisheng Jianyan Zazhi 17(12) (2007), 2244-2246.
22. Korhonen, J. M.; Sclivagnotis, Y.; von Wright, A Characterization of dominant cultivable lactobacilli and their antiobiotic resistance profiles from faecal samples of weaning piglets. . Journal of Applied Microbiology, 103(6), (2007). 2496-2503.
23. Lyskova, P.; Vydrzalova, M.; Mazurova, J, Identification and antimicrobial susceptibility of bacteria and yeasts isolated from healthy dogs and dogs with otitis externa,. Journal of Veterinary Medicine, A: Physiology, Pathology, Clinical Medicine, 54(10), (2007), 559-563.
24. Starner, Timothy D.; Shrout, Joshua D.; Parsek, Matthew R.; Appelbaum, Peter C.; Kim, GunHee. Sub inhibitory concentrations of azithromycin decrease noticeable Haemophilus influenza biofilm formation and diminish established, Antimicrobial Agents and Chemotherapy, 52(1), (2008),137-145.
25. Miranda, J. M.; Vazquez, B. I.; Fente, C. A.; Barros-Velazquez, J.; Cepeda, A, Franco Abuin, C. M , Antimicrobial resistance in Escherichia coli strains isolated from organic and conventional pork meat: a comparative survey, European Food Research and Technology,226,(3), (2008), 371-375.
26. Selke-Krulichova, Iva; Martinkova, Jirina; Pokorna, Pavla; Zahora, Jiri. Therapeutic drug monitoring (TDM) of gentamicin in critically ill neonate, Biomedical Papers 151(Suppl. 1), (2007), 84-86.
27. Helling, Kai; Schoenfeld, Uwe; Clarke, Andrew H Treatment of Meniere's disease by low-dosage intratympanic gentamicin application: effect on otolith function. Laryngoscope, 117(12), (2007). 2244-2250.
28. Maudonnet, Eloisa Nogueira; de Oliveira, Jose Antonio A.; Rossato, Maria; Hyppolito, Miguel Angel Gentamicin Attenuates Gentamicin-Induced Ototoxicity - Self-Protectiono. Drug and Chemical Toxicology 31(1), (2008), 11-25.
29. Coats, A.W and J.P. Redfern, Nature, 201,68,(1964)
30. R.Shirly, The CRYSFIRE System for Automayic powder Indexing: Users manual,Lattice press, Guilford, UK(2002).
31. Horacio, López-Sandoval, Milton E. Londoño-Lemos, Raúl Garza-Velasco, Israel Poblano-Meléndez, Pilar Granada-Macías, Isabel Gracia-Mora, Norah Barba-Behre Synthesis, structure and biological activities of cobalt(II) and zinc(II) coordination compounds with 2-benzimidazole

derivatives, Journal of Inorganic Biochemistry, 102, (2008), 5-6, 1267-1276.

32. R. Di Stefano, M. Scopelliti, C. Pellerito, G. Casella, T. Fiore, G.C. Stocco, R. Vitturi, M. Colomba, L. Ronconi, I.D. Sciacca, L. Pellerito Organometallic complexes with biological molecules. XVIII. Alkyltin(IV) cephalexinate complexes: synthesis, solid state and solution phase investigations Journal of Inorganic Biochemistry, 98, (2009), 3, 534-546.

33. R. Di Stefano, M. Scopelliti, C. Pellerito, T. Fiore, R. Vitturi, M. S. Colomba, P. Gianguzza, G. C. Stocco, M. Consiglio, L. Pelleri Organometallic complexes with biological molecules: XVII. Triorganotin(IV) complexes with amoxicillin and ampicillin Journal of Inorganic Biochemistry, 89, (2009)3-4,279-292.

****